Soliton synchronization in microresonators with a modulated pump

Jorge Palacio Mizrahi,[1] Logan Courtright,[2] Pradyoth Shandilya,[2] Curtis R. Menyuk,[2] and Omri Gat[1,*]
[1]*The Racah Institute of Physics, The Hebrew University of Jerusalem, Jerusalem 9190401, Israel*
[2]*Computer Science and Electrical Engineering Department, University of Maryland at Baltimore County, 1000 Hilltop Circle, Baltimore, Maryland 21250, USA*

(Received 7 December 2023; accepted 2 April 2024; published 5 June 2024)

Microresonator frequency comb generation from Kerr solitons has become a cutting edge technology, but challenges remain in creating, maintaining, and controlling the solitons. Pump modulation and dual pumping are promising techniques for meeting these challenges. Here we derive the equation of motion of solitons interacting with a modulated pump in the framework of synchronization theory. It implies that the soliton repetition rate locks to the modulation frequency whenever the latter is within a locking range of frequencies around an integer multiple of the free spectral range of the microresonator. We calculate explicitly, numerically, and in perturbation theory the width of the locking range as a function of the amplitude and frequency of the pump and the modulation phase. We show that a highly red-detuned, strong pump that is amplitude-modulated provides the best conditions for entrainment, and that the width of the locking range is proportional to the square of the modulation frequency, limiting the effectiveness of RF modulation as an entrainment method.

DOI: 10.1103/PhysRevE.109.064204

I. INTRODUCTION

Generation of frequency combs from dissipative solitons in Kerr microresonators is an important technology with numerous applications [1–3]. A standard method for obtaining microresonator solitons is to pump the microresonator with a single continuous wave (CW) near a resonance, and reduce (red detune) the pump frequency. The optical field in the microresonator then loses stability, becomes time dependent and chaotic, before finally settling into a soliton waveform [4]. This approach suffers from serious drawbacks, including thermal instabilities [5] and nondeterministic operation.

One way to facilitate the generation of solitons is to modulate the pump periodically, breaking the inherent time-translation symmetry. Several variations of this idea have been studied: The pump can be modulated electrooptically, creating spectral sidebands around the main pump line [6–11]; it can be coherently mixed with a second pump, creating a periodic beat pattern [12], an effect that has been used to synthesize soliton crystals [13]. Alternatively, the pump can be combined with pulses from an external source [14–16], an approach that is also suitable for other types of Kerr resonators [17–20].

The pump modulation protocols excite soliton waveforms by a resonant process that becomes effective when the modulation frequency is close to a rational multiple of the free spectral range. The repetition rate of the soliton waveform is then entrained to the pump modulation frequency; it is a manifestation of the synchronization phenomenon of nonlinear dynamics wherein the frequencies of coupled self-sustained oscillators are locked in a rational proportion [21]. Since the entrainment is stable in a finite interval of detunings, the pump modulation frequency can be used as a knob to tune the soliton repetition rate as long as synchronization is maintained. A similar synchronization mechanism can be used to lock the frequencies of two solitons that are counter-propagating in the same cavity [22,23] or in two coupled cavities [24,25].

When the pump modulation is shallow, the soliton shape is only slightly distorted, and the modulation couples to the soliton repetition rate mainly through the zero mode of its stability spectrum associated with translation symmetry [26]. This is the universal mechanism of interaction of localized coherent structures, such as kinks, pulses, and vortices with external fields that are not strong enough to strongly deform them. The coupling to the translational zero mode has been extensively used to study the effective force external fields exert on dissipative solitons and other localized coherent structure, see, e.g., [27–31].

In this paper, we calculate the effective soliton motion imposed by pump modulation, and use it to determine how far the repetition rate of the entrained soliton can be pulled away from the free soliton repetition rate. In other words, what is the range of modulation frequencies that can lock the soliton repetition rate?

This question is fundamental in the theory of synchronization of self-sustained oscillators [21]. It follows from this theory that the range of frequencies where entrainment occurs is determined by a locking dynamical system that governs the time evolution of the phases of the coupled oscillators. The entrained steady states appear as fixed points of the locking dynamical system, and the locking range consists of the parameter values for which there are stable entrainment fixed points.

Here we focus on the entrainment of a Kerr soliton by a sinusoidally modulated pump. Our first main result, derived in Sec. II, is the equation of motion of the pulse center in

*omrigat@mail.huji.ac.il

the frame where the pump field is stationary, which turns out to be an Adler equation [21]. As usual in the entrainment of pulses [18,32], the locking amplitude is equal to the projection of the pump modulation signal on the adjoint zero mode associated with translation symmetry spontaneously broken by the Kerr soliton, which is directly proportional to the modulation depth.

In Sec. III we calculate explicitly the locking range using two methods. In Sec. III A, the soliton and the associated adjoint zero mode are calculated numerically for the values of pump amplitude and detuning supporting soliton steady states, and use them to calculate the locking range for amplitude- and phase-modulated pumps. We next calculate, for each choice of pump parameters, the optimal modulation phase which maximizes the width of the locking range, and the maximal width, concluding that the conditions that facilitate entrainment are obtained for a strong pump that is highly detuned and amplitude modulated.

In Sec. III B we focus on the case of the highly detuned pump, and study it in perturbation theory. We show that the locking range width increases without bound as the pump is further red detuned; however, exciting solitons and maintaining them becomes increasingly harder in this limit, where an increasingly strong pump is needed, and the conversion efficiency is low.

The entrainment of microresonator solitons by an RF-modulated pump was studied experimentally in [10], revealing a locking range of about 1 KHz or less that is very narrow compared with the free spectral range of more than 13 GHz. In Sec. IV we conclude that the fragility of entrainment is an inherent limitation of this locking mechanism, tied to the large separation of scales between the soliton bandwidth and the RF scale, and suggest more robust entrainment methods.

II. SYNCHRONIZATION TO A MODULATED PUMP

A. The wave equation

Our dynamical model for the cavity field ψ is based on the standard Lugiato-Lefever equation (LLE) with second-order dispersion

$$\frac{\partial\psi}{\partial t} = -\left(\frac{l}{2} + i\alpha\right)\psi + \frac{i\beta}{2}\frac{\partial^2\psi}{\partial x^2} + i\gamma|\psi|^2\psi + f, \qquad (1)$$

where, l, α, β, γ, and f are, respectively, the linear loss rate, pump detuning, second-order dispersion coefficient, Kerr coefficient, and pump amplitude; $0 \leqslant x \leqslant L$ is the azimuthal position along the resonator with periodic boundary condition, and t is time.

We assume that the pump is sinusoidically modulated with frequency ν_M, and therefore let [7]

$$f = f_0\left(1 + \varepsilon e^{i\theta}\cos\left(\frac{2\pi n}{L}x - 2\pi(\nu_M - n\nu_{\mathrm{FSR}})t\right)\right), \qquad (2)$$

where the constant f_0 is the mean pump amplitude, $\varepsilon > 0$ is the modulation depth, assumed small, and θ the modulation phase, with $\theta = 0$ corresponding to amplitude modulation (AM), and $\theta = \pi/2$ corresponding to phase modulation (PM). We assume that ν_M is close to an integer multiple, n, of the free spectral range, ν_{FSR}, so that the detuning is small: $|\nu_M - n\nu_{\mathrm{FSR}}| \ll \nu_{\mathrm{FSR}}$.

We next make (1) dimensionless by choosing natural units $1/(2\alpha)$, $\sqrt{\beta/(2\alpha)}$, and $\sqrt{2\alpha/\gamma}$ of time, position, and amplitude, respectively, obtaining

$$\frac{\partial\psi}{\partial t} = N\psi + \varepsilon M, \qquad (3)$$

$$N\psi = -\left(\delta + \frac{i}{2}\right)\psi + \frac{i}{2}\frac{\partial^2\psi}{\partial x^2} + i|\psi|^2\psi - \frac{i}{2}h, \qquad (4)$$

$$M = -\frac{i}{2}he^{i\theta}\cos(b(x - vt)), \qquad (5)$$

with $\delta = l/(4\alpha)$, $h = i\sqrt{\gamma/(2\alpha^3)}f_0$, $b = 2\pi\sqrt{\beta/2\alpha}\,n/L$, and $bv = 2\pi(\nu_M - n\nu_{\mathrm{FSR}})/(2\alpha)$. The choice of a dimensionless form with a normalized detuning coefficient in Eq. (4) (instead of the more common normalized loss) facilitates calculations with large detunings, where δ is small.

When there is no modulation, i.e., when $\varepsilon = 0$, the LLE (3) has stable stationary pulse solutions $\psi_s(x)$ for suitable values of the parameters, which correspond to a Kerr soliton propagating with group velocity $\nu_{\mathrm{FSR}}L$ in the microresonator [33]. When the modulation is turned on and v is nonzero, there is a mismatch between the modulation frequency and the group velocity of the free soliton. Synchronization theory implies that there is a range of values of v where the soliton is entrained by the modulation and travels at velocity $\nu_M L/n$ [21]. When v is outside this range, Eq. (3) has no stationary solutions, and the output waveform is quasiperiodic. Our goal is to calculate the locking range of v for which the soliton is entrained.

B. The role of translation symmetry

Entrainment of solitons is facilitated by the symmetry under translation of the unmodulated LLE, which implies that when $\psi_s(x)$ is a stationary solution of this equation, so is $\psi_s(x - \xi)$ for any real ξ. The pump modulation couples with the translational degree of freedom of the pulse via the zero mode in the stability spectrum of the pulse associated with translation symmetry, as we explain next [26].

Stability of solutions of the LLE is conveniently addressed in a doubled phase space of a vector-valued field $\Psi = (\psi, \psi^*)$, where * stands for complex conjugation, which satisfies the equation

$$\frac{\partial\Psi}{\partial t} = \mathcal{N}\Psi + \varepsilon\mathcal{M}, \qquad (6)$$

where

$$\mathcal{N}\Psi = (N\psi,\ (N\psi)^*), \quad \mathcal{M} = (M,\ M^*). \qquad (7)$$

The operator governing the linear stability of the LLE soliton is

$$\mathcal{L} \equiv (\partial_\Psi\mathcal{N})|_{\Psi_s} = \begin{pmatrix} A & B \\ B^* & A^* \end{pmatrix}, \qquad (8)$$

$$A = (\partial_\psi N)|_{\psi_s} = -\left(\delta + \frac{i}{2}\right) + \frac{i}{2}\frac{\partial^2}{\partial x^2} + 2i|\psi_s|^2, \qquad (9)$$

$$B = (\partial_{\psi^*}N)\big|_{\psi_s} = i\psi_s^2, \qquad (10)$$

and the translation symmetry implies that $\mathcal{N}\Psi_s(x-\xi)=0$ for all ξ, so that

$$0=\frac{d}{d\xi}\mathcal{N}\Psi_s(x-\xi)|_{\xi=0}=\mathcal{L}\Psi_\xi,\quad \Psi_\xi=-\frac{d\Psi_s}{dx}; \tag{11}$$

Ψ_ξ is the translational zero mode.

The soliton position ξ becomes time dependent when the pump is modulated, i.e., when $\varepsilon>0$, and the next step is to find the equation of motion that governs the dynamics of $\xi(t)$. In addition to shifting the pulse position, the pump modulation distorts its shape, so that we write the solution of (6) in the form

$$\Psi(x,t)=\Psi_s(x-\xi(t))+\varepsilon\Psi_1(x-\xi(t),t)+\mathcal{O}(\varepsilon^2). \tag{12}$$

Under the assumption of weak modulation, the soliton distortion $\varepsilon\Psi_1$ is small; nevertheless, its presence means that without additional specification $\xi(t)$ is not precisely defined, since it can be slightly changed, keeping the same Ψ in (12), with the help of a suitable change in Ψ_1. We eliminate this ambiguity by imposing the condition that the expansion of Ψ_1 in eigenfunctions of $\mathcal{L}$ has no component along the eigenvector Ψ_ξ. This condition can be imposed by requiring that

$$\langle\bar{\Psi}_\xi,\Psi_1\rangle=0, \tag{13}$$

where the inner product is

$$\left\langle\begin{pmatrix}\phi_1\\ \phi_2\end{pmatrix},\begin{pmatrix}\psi_1\\ \psi_2\end{pmatrix}\right\rangle=\frac{1}{2}\int_{-\infty}^{\infty}(\phi_1^*\psi_1+\phi_2^*\psi_2)dx, \tag{14}$$

and $\bar{\Psi}_\xi=(\bar{\psi}_\xi,\bar{\psi}_\xi^*)$ is the zero mode of the adjoint of $\mathcal{L}^\dagger$ of $\mathcal{L}$ associated with Ψ_ξ,

$$\mathcal{L}^\dagger\bar{\Psi}_\xi=0,\quad \mathcal{L}^\dagger=\begin{pmatrix}A^* & B\\ B^* & A\end{pmatrix}, \tag{15}$$

normalized such that

$$\langle\bar{\Psi}_\xi,\Psi_\xi\rangle=1. \tag{16}$$

Substituting Eq. (12) in Eq. (6), and neglecting terms of order $\mathcal{O}(\varepsilon^2)$ leads to

$$\Psi_\xi\frac{d\xi}{dt}+\varepsilon\frac{d\Psi_1}{dt}=\mathcal{L}\Psi_1+\varepsilon\mathcal{M}. \tag{17}$$

Projecting this equation on $\bar{\Psi}_\xi$ and using (15) then yields the equation of motion for the pulse position

$$\frac{d\xi}{dt}=\varepsilon\langle\bar{\Psi}_\xi,\mathcal{M}\rangle. \tag{18}$$

C. The locking dynamics

The right-hand side of Eq. (18) depends explicitly on time, but we can write an autonomous equation of motion for the soliton position in the frame where the modulation is stationary, $y=\xi-vt$,

$$\frac{dy}{dt}=-v+\frac{1}{2}\varepsilon\mathrm{Im}\left(he^{i\theta}\int_{-\infty}^{\infty}\bar{\psi}_\xi^*(z)\cos[b(z+y)]dz\right); \tag{19}$$

a stationary solution of this equation corresponds to an entrained-soliton steady-state waveform.

Since $\bar{\psi}_\xi$ is odd, we can rewrite Eq. (19) in the form

$$\frac{dy}{dt}=-v+W\sin(by), \tag{20}$$

where

$$W=-\frac{1}{2}\varepsilon\mathrm{Im}\left(he^{i\theta}\int_{-\infty}^{\infty}\bar{\psi}_\xi^*(z)\sin(bz)dz\right). \tag{21}$$

Equation (20) is a form of the Adler equation of synchronization theory [21], exhibiting a sharp threshold: When $|v|<|W|$, the soliton becomes entrained and y tends to the limiting value $(\pi-\arcsin(v/W))/b$ for positive W or $\arcsin(v/W))/b$ for negative W, whereas when $|v|\geqslant|W|$, $|y|$ grows in time without limit, and the waveform evolution is quasiperiodic. Hence, the width of the locking range of modulation frequencies in which entrainment is possible is equal to $2|W|$, and the sign of W determines whether the pulse leads or trails the peak of the modulation. It follows directly from Eq. (21) that the width of the locking range is proportional to the modulation depth.

Next we note that the normalized modulation wave number b is comparable with the ratio of the pulse duration and the modulation period, which is small in typical microresonator experiments. The zero-mode $\bar{\psi}_\xi$ is localized and decays to zero on an order-one scale of the normalized units, so that $b\ll 1$, implying that Eq. (21) can be simplified by approximating the sine by its behavior for small argument $\sin(bz)\sim bz$. It follows that

$$W=-\frac{1}{2}\varepsilon b\mathrm{Im}(e^{i\theta}w),\quad w=h\int_{-\infty}^{\infty}z\bar{\psi}_\xi^*(z)dz. \tag{22}$$

This expression displays explicitly the dependence of the locking range semiwidth W on the modulation parameters, ε, b, and θ, making it possible to focus our attention on the normalized width w that depends only on the cavity and pump parameters δ and h.

Equation (22) implies that for fixed pump parameters, the modulation depth W is $O(b)$ for $b\ll 1$. Recall (Sec. II A) that the detuning between the modulation frequency and the nth harmonic of the FSR is directly proportional to b and the disparity parameter v. Hence, the frequency locking range is $O(b^2)$, i.e., much smaller than the free spectral range.

III. CALCULATION OF THE LOCKING RANGE

As shown above, Eq. (22), the locking range depends on the soliton waveform only through the normalized width w that is a complex-valued function of the parameters δ, h. It can be expressed as $w=-w_{\mathrm{PM}}+iw_{\mathrm{AM}}$, where the real normalized widths w_{PM}, w_{AM}, are proportional to the signed semiwidth W with phase-modulated and amplitude-modulated pump, respectively. Expressing the polar representation of the normalized width as $w=w_{\mathrm{opt}}\exp(-i(\pi/2+\theta_{\mathrm{opt}}))$, θ_{opt} is the modulation phase that maximizes W, and w_{opt} is proportional to the $\max_\theta(W)$ that is obtained if θ_{opt} is chosen as the modulation phase.

A. Numerical calculation

We approach the calculation of the normalized width using two methods. In this subsection we present the results of the numerical approach. The calculation consists of three steps. (i) The unmodulated-pump operator N of the LLE defined in Eq. (4) is discretized using finite differences, yielding a set of nonlinear functions; using a root finding algorithm, we

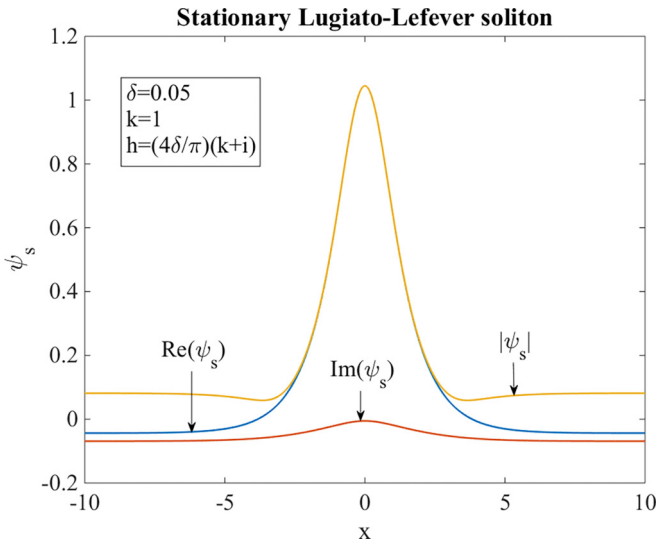

FIG. 1. A numerically calculated stable soliton solution of the unmodulated LLE with normalized loss parameter $\delta = 0.05$, and an unmodulated pump amplitude $h = (4\delta/\pi)(1 + i)$.

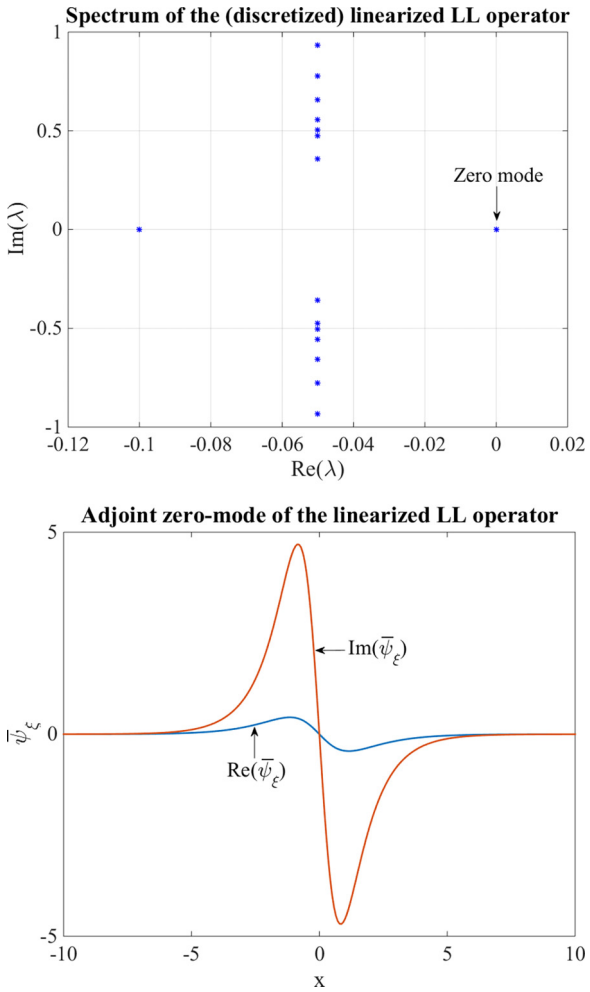

FIG. 2. Top: Part of the spectrum of the discretized LLE soliton stability operator. There is one zero eigenvalue, corresponding to Ψ_ξ, the translation mode. Bottom: The numerically calculated adjoint zero-mode eigenfunction $\bar{\psi}_\xi$. Pump parameters as in Fig. 1.

calculate a discretized version of the LLE soliton. (ii) We calculate the linear stability matrix of the discretized operator, obtaining a discretized version of the LLE stability operator $\mathcal{L}$; then we calculate the eigenvalues, checking the soliton stability, and obtain a discretized version of the adjoint zero mode, normalized according to Eq. (16). (iii) We calculate the integral in Eq. (22) using numerical quadrature. Examples of intermediate results obtained in steps (i) and (ii) are shown in Figs. 1 and 2, respectively.

We next note that like the standard LLE, the modulated-pump LLE is symmetric under a combined phase shift of the field and pump. That is, if $\psi(x,t)$ is a solution of Eq. (3) with pump amplitude h, then $e^{i\phi}\psi(x,t)$ is a solution with pump amplitude $e^{i\phi}h$, for any real phase shift ϕ. It follows that the locking range depends only on the modulus of h, so that without loss of generality we can choose the pump phase such that $h = h_r + (4\delta/\pi)i$, $h_r > 0$, a choice that guarantees the existence of stable solitons for small δ, $|h|$ [33], and is convenient for comparing the numerical and perturbative calculations of the locking range.

The results of the calculation of the width are shown in Fig. 3. The shaded regions correspond to the δ, h_r combinations for which there exist a soliton solution. For $\delta < 0.16$ the LL soliton becomes unstable through a Hopf bifurcation when h_r surpasses some positive threshold [33]. The locking range calculation is well defined for the unstable solitons, and is arguably applicable to experiments where the solitons are stabilized by the pump modulation. We display the results in the unstable region in Fig. 3 using lighter shades to distinguish it from the stable region.

Some interesting qualitative conclusions can be drawn from the numerical results. The most striking feature is the broadening of the locking range for small δ, where $w_{\rm opt} \approx 9$ for $\delta = 0.01$, h_i near the Hopf stability boundary, and reaches values larger than 30 for Hopf unstable solitons. The perturbative analysis of the next section suggests that $w_{\rm opt}$ grows linearly with detuning (i.e., as $1/\delta$) for highly detuned pump with constant h_r.

Wide locking ranges can be achieved for AM pump with $w_{\rm AM}$ significantly larger than one, while $w_{\rm PM}$ is close to two for all soliton pump parameters. On the other hand, $w_{\rm AM}$ depends strongly on δ, h_r, and changes sign on a curve in the middle of the soliton stability region, shown in dashed gray in the top right panel of Fig. 3. Moderately large values of $w_{\rm opt} \approx 5$ are also obtained for large δ and small h_r solitons.

B. Perturbative calculation for large detuning

In this section we calculate w in the limit

$$\delta \to 0, \quad h = (k + i)4\delta/\pi \tag{23}$$

with k fixed. In this limit, the LLE (3) approaches the nonlinear Schrodinger equation (NLSE). However, since the limit is singular, one cannot simply calculate the locking range on the basis of the NLS soliton $\Psi_{s,0}$ and its zero-eignevalue stability modes. Indeed, unlike the LLE, the subspace associated with the zero eigenvalue of the NLSE stability operator $\mathcal{L}_0$ is four-dimensional, the direct sum of a subspace spanned by

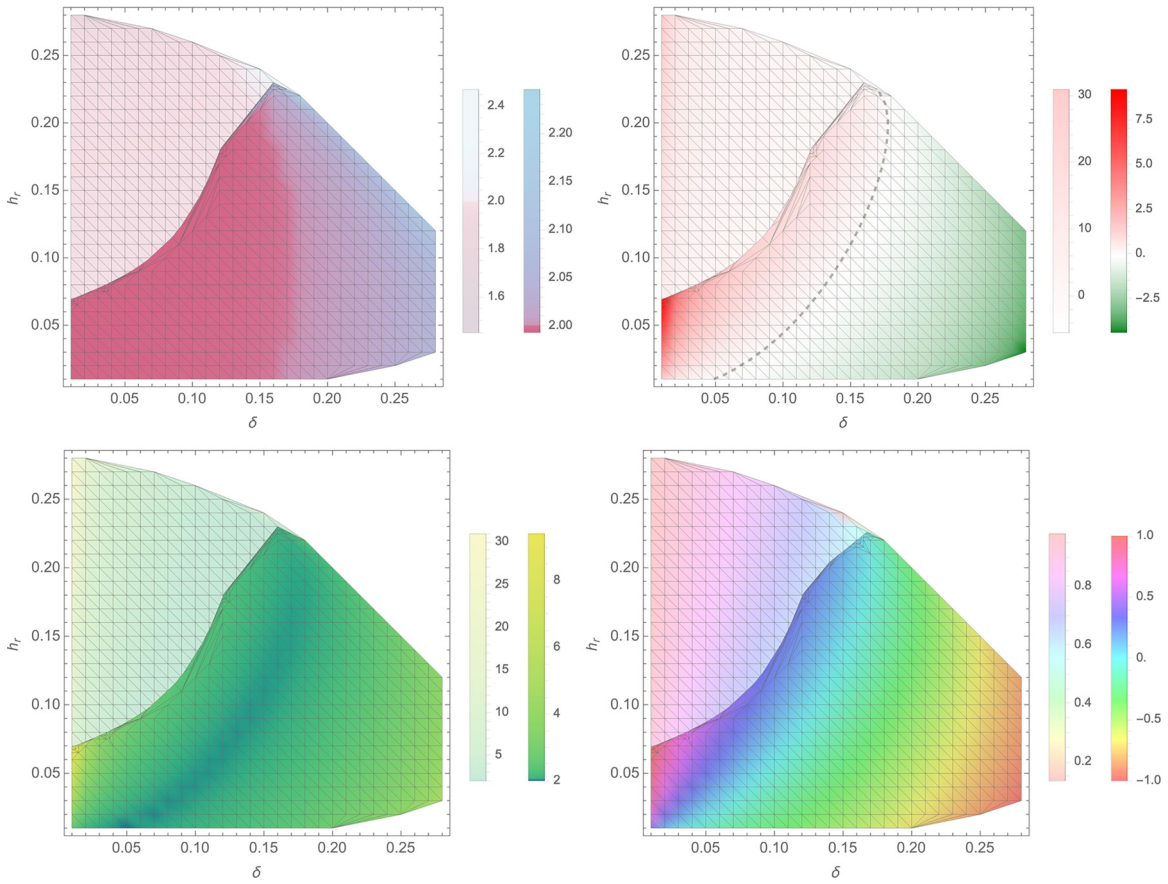

FIG. 3. Normalized locking range for solitons of the LLE with normalized loss δ and pump amplitide $h_r + (4\delta/\pi)i$. Soliton solutions of the unmodulated-pump LLE exist in the colored region of each panel. The solutions are stable in the heavily shaded regions and are subject to breathing instability in the light shaded regions. From left to right, top to bottom, the panels show $w_{\rm PM}$, $w_{\rm AM}$, $w_{\rm opt}$, and $\theta_{\rm opt}/\pi$. $w_{\rm AM} = 0$ along the dashed curve in the top-right panel. The right-most color (shade) bar in each panel corresponds to the stable region, while the bar to its left corresponds to the unstable region. In both the top-right and bottom-right panels (showing $w_{\rm AM}$ and $\theta_{\rm opt}/\pi$, respectively), positive values are obtained for small δ (left parts of the figure) and negative values are obtained for large δ (right parts).

an even eigenfunction and an even generalized eigenfunction, and a subspace spanned by an odd eigenfunction and an odd generalized eigenfunction [34]. The adjoint NLSE stability operator has corresponding (generalized) eigenfunctions with corresponding parity symmetries.

The singular perturbation theory of the LLE soliton direct and adjoint stability problems is elaborate, and in this section we use the results that are necessary for our present purpose, deferring a complete presentation to a forthcoming publication. In the limit given by Eq. (23) $\psi_s \sim \psi_{s,0} + \delta\psi_{s,1}$, $\psi_{s,0}(x) = \mathrm{sech}(x)$, and the linear stability operator $\mathcal{L} \sim \mathcal{L}_0 + \delta\mathcal{L}_1$, with

$$\mathcal{L}_0 = \begin{pmatrix} A_0 & B_0 \\ B_0^* & A_0^* \end{pmatrix}, \tag{24}$$

$$A_0 = -\frac{i}{2} + \frac{i}{2}\frac{\partial^2}{\partial x^2} + 2i|\psi_{s,0}|^2, \quad B_0 = i\psi_{s,0}^2, \tag{25}$$

and

$$\mathcal{L}_1 = \begin{pmatrix} A_1 & B_1 \\ B_1^* & A_1^* \end{pmatrix}, \tag{26}$$

$$A_1 = 4i\mathrm{Re}(\psi_{s,0}^*\psi_{s,1}), \quad B_1 = 2i\psi_{s,0}\psi_{s,1}. \tag{27}$$

To leading order, the LLE translational zero mode and its adjoint are in the odd NLSE zero subspaces. The odd zero subspace of $\mathcal{L}_0$ is spanned by

$$\Psi_{\xi,0} = (\psi_{\xi,0}, \psi_{\xi,0}^*), \quad \psi_{\xi,0}(x) = \mathrm{sech}(x)\tanh(x) \tag{28}$$

and

$$\Psi_{k,0} = (\psi_{k,0}, \psi_{k,0}^*), \quad \psi_{k,0}(x) = ix\,\mathrm{sech}(x), \tag{29}$$

which satisfy

$$\mathcal{L}_0\Psi_{\xi,0} = 0, \quad \mathcal{L}_0\Psi_{k,0} = \Psi_{\xi,0}, \tag{30}$$

and the odd zero subspace of $\mathcal{L}_0^\dagger$ is spanned by

$$\bar{\Psi}_{\xi,0} = (\bar{\psi}_{\xi,0}, \bar{\psi}_{\xi,0}^*), \quad \bar{\psi}_{\xi,0} = -i\psi_{k,0} \tag{31}$$

and

$$\bar{\Psi}_{k,0} = (\bar{\psi}_{k,0}, \bar{\psi}_{k,0}^*), \quad \bar{\psi}_{k,0} = i\psi_{\xi,0}, \tag{32}$$

satisfying

$$\mathcal{L}_0^\dagger\bar{\Psi}_{k,0} = 0, \quad \mathcal{L}_0^\dagger\bar{\Psi}_{\xi,0} = \bar{\Psi}_{k,0}. \tag{33}$$

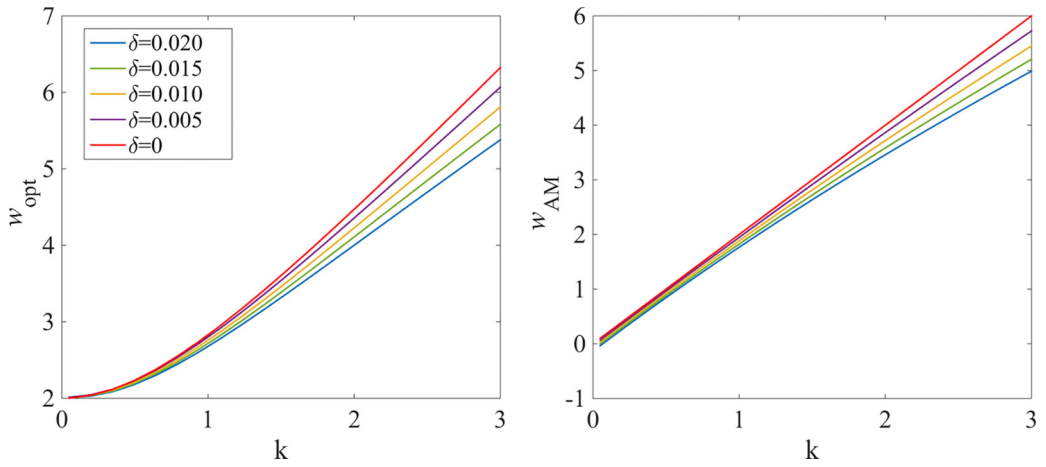

FIG. 4. The normalized locking width with optimal pump phase (left) and amplitude modulation (right), shown for several small values of normalized loss δ as a function of normalized pump amplitude $h = (k + i)4\delta/\pi$; the values of δ increase from the top to the bottom curves. The $\delta = 0$ curves show the perturbative results of Eqs. (39) and (40), and the $\delta > 0$ curves show numerical results, that are well approximated by perturbation for the displayed range of δ and k.

The adjoint basis functions are normalized such that they obey the biorthogonality relations

$$\langle \bar{\Psi}_{\xi,0}, \Psi_{\xi,0} \rangle = \langle \bar{\Psi}_{k,0}, \Psi_{k,0} \rangle = 1, \tag{34}$$

$$\langle \bar{\Psi}_{\xi,0}, \Psi_{k,0} \rangle = \langle \bar{\Psi}_{k}, \Psi_{\xi,0} \rangle = 0. \tag{35}$$

In the limit (23) the direct and adjoint LLE zero modes asymptotics are

$$\Psi_{\xi} \sim \Psi_{\xi,0} - \delta \langle \bar{\Psi}_{\xi,0}, \mathcal{L}_1 \Psi_{\xi,0} \rangle \Psi_{k,0}, \tag{36}$$

$$\bar{\Psi}_{\xi} \sim -\frac{1}{2} \langle \bar{\Psi}_{k,0}, \mathcal{L}_1 \Psi_{k,0} \rangle \bar{\Psi}_{\xi,0} + \frac{1}{2\delta} \bar{\Psi}_{k,0}. \tag{37}$$

We observe that as a singular perturbation, $\bar{\Psi}_{\xi}$ does not approach $\bar{\Psi}_{\xi,0}$ as $\delta \to 0$. Instead, it diverges as $1/\delta$, a behavior that can be traced to the algebraic degeneracy of the zero eigenvalue of the NLSE stability operator, and its splitting in the spectrum of the LLE stability operator.

Recall [Eq. (22)] that the normalized locking range w is proportional to the normalized pump amplitude h that tends to zero in the limit given by Eq. (23), canceling the divergence of $\bar{\Psi}_{\xi}$ as $\delta \to 0$, yielding the finite limiting value

$$w \sim \frac{h}{2\delta} \int_{-\infty}^{\infty} z \tanh z \operatorname{sech} z dz = -2 + 2ik, \tag{38}$$

so that

$$w_{\mathrm{AM}} \sim 2k, \quad w_{\mathrm{PM}} \sim 2 \tag{39}$$

and

$$w_{\mathrm{opt}} \sim 2\sqrt{1 + k^2}, \quad \theta_{\mathrm{opt}} \sim \arctan\left(\frac{1}{k}\right). \tag{40}$$

Figures 4 and 5 compare the expressions (39) for the normalized locking range widths w_{opt}, w_{AM}, and (40) for optimal pump phase θ_{opt} in the limit given by Eq. (23), with the numerical results for small but finite δ. Evidently, the limiting values provide an excellent approximation for the locking range with large detunings; the small δ numerical results for w_{PM} (not shown) are consistent with Eq. (39) and exhibit no dependence on k within our numerical accuracy.

The most significant implication of the perturbative analysis is that the broadest locking range is obtained in the limit of large detunings for large k with an amplitude-modulated pump. This result is consistent with the numerical calculations of Sec. III A, where we found that the locking range width becomes large for small δ and large $|h|$.

IV. CONCLUSIONS

Pump modulation in Kerr microresonators has been proposed and implemented as a method to control and stabilize Kerr solitons. We show that this effect is an example of the universal synchronization phenomenon in nonlinear dynamics. Starting from the modulated-pump LLE, we derive the Adler equation that governs the soliton entrainment dynamics.

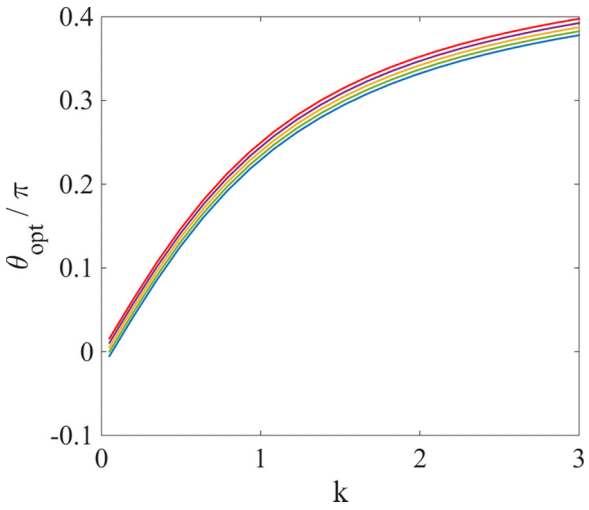

FIG. 5. The optimal pump phase for system parameters as in Fig. 4, with the same curve labeling scheme as a function of δ, increasing from top to bottom.

We then use this equation to find the conditions under which the pulse repetition rate will lock to the pump modulation frequency, showing that the width of the locking range grows linearly with the modulation depth. It follows from the Adler equation that when the soliton repetition rate is unlocked, it is still pulled toward the modulation frequency, resulting in quasiperiodic oscillations [21], as seen in the experiments of [10].

A striking feature in these experiments is that the locking range is very narrow, less than 1 KHz around a base frequency of more than 10 GHz. The narrowness of the locking range stems from the large separation between the picosecond-scale soliton width and the nanosecond-scale cavity roundtrip time. The pump modulation is gradient coupled to the pulse, so that the scale separation leads to weak coupling. A more subtle effect of the scale separation is that it translates a small detuning of frequencies to a large disparity in the group velocities.

We showed that, as a consequence, the locking range increases quadratically with the frequency of the pump modulation. Hence, the locking range can be widened by a large factor by modulating the pump near a large harmonic n of the pulse repetition rate, but the values of n reachable with RF modulation are limited in practice. Nevertheless, this idea can be realized using dual pumping, with a secondary pump detuned by hundreds of GHz with respect to the primary pump.

Less dramatic but still significant variations of the locking range width are obtained as the pump parameters and the modulation phase are changed. When the pump is phase modulated, we find that the normalized locking range depends very weakly on the pump amplitude and detuning. By contrast, when the pump amplitude is modulated, the width varies between zero along a curve in the space of pump parameters to large values in the limit of large detunings. We showed using perturbation theory that the large-detuning limit is singular, causing the coupling between the pump modulation and the soliton to be enhanced by a factor proportional to the detuning. Here pump power is liable to be the limiting practical factor, since maintaining soliton operation requires an increasingly large pump amplitude as detuning increases.

ACKNOWLEDGMENTS

J.P.M. and O.G. thank the US-Israel Binational Science Foundation for financial support under NSF-BSF Grant No. 2017643. L.C., P.S., and C.R.M. thank the National Science Foundation for financial support under Grant No. ECCS-1807272.

[1] T. J. Kippenberg, A. L. Gaeta, M. Lipson, and M. L. Gorodetsky, Dissipative Kerr solitons in optical microresonators, Science **361**, eaan8083 (2018).

[2] S. A. Diddams, K. Vahala, and T. Udem, Optical frequency combs: Coherently uniting the electromagnetic spectrum, Science **369**, eaay3676 (2020).

[3] B. Shen, L. Chang, J. Liu, H. Wang, Q.-F. Yang, C. Xiang, R. N. Wang, J. He, T. Liu, W. Xie, J. Guo, D. Kinghorn, L. Wu, Q.-X. Ji, T. J. Kippenberg, K. Vahala, and J. E. Bowers, Integrated turnkey soliton microcombs, Nature (London) **582**, 365 (2020).

[4] T. Herr, V. Brasch, J. D. Jost, C. Y. Wang, N. M. Kondratiev, M. L. Gorodetsky, and T. J. Kippenberg, Temporal solitons in optical microresonators, Nat. Photonics **8**, 145 (2014).

[5] Q. Li, T. C. Briles, D. A. Westly, T. E. Drake, J. R. Stone, B. R. Ilic, S. A. Diddams, S. B. Papp, and K. Srinivasan, Stably accessing octave-spanning microresonator frequency combs in the soliton regime, Optica **4**, 193 (2017).

[6] S. B. Papp, P. Del'Haye, and S. A. Diddams, Parametric seeding of a microresonator optical frequency comb, Opt. Express **21**, 17615 (2013).

[7] H. Taheri, A. A. Eftekhar, K. Wiesenfeld, and A. Adibi, Soliton formation in whispering-gallery-mode resonators via input phase modulation, IEEE Photonics Journal **7**, 1 (2015).

[8] V. E. Lobanov, G. V. Lihachev, N. G. Pavlov, A. V. Cherenkov, T. J. Kippenberg, and M. L. Gorodetsky, Harmonization of chaos into a soliton in Kerr frequency combs, Opt. Express **24**, 27382 (2016).

[9] D. C. Cole, J. R. Stone, M. Erkintalo, K. Y. Yang, X. Yi, K. J. Vahala, and S. B. Papp, Kerr-microresonator solitons from a chirped background, Optica **5**, 1304 (2018).

[10] W. Weng, E. Lucas, G. Lihachev, V. E. Lobanov, H. Guo, M. L. Gorodetsky, and T. J. Kippenberg, Spectral purification of microwave signals with disciplined dissipative Kerr solitons, Phys. Rev. Lett. **122**, 013902 (2019).

[11] W. Weng, J. He, A. Kaszubowska-Anandarajah, P. M. Anandarajah, and T. J. Kippenberg, Microresonator dissipative Kerr solitons synchronized to an optoelectronic oscillator, Phys. Rev. Appl. **17**, 024030 (2022).

[12] H. Taheri, A. B. Matsko, and L. Maleki, Optical lattice trap for Kerr solitons, Eur. Phys. J. D **71**, 153 (2017).

[13] Z. Lu, H.-J. Chen, W. Wang, L. Yao, Y. Wang, Y. Yu, B. E. Little, S. T. Chu, Q. Gong, W. Zhao, X. Yi, Y.-F. Xiao, and W. Zhang, Synthesized soliton crystals, Nat. Commun. **12**, 3179 (2021).

[14] E. Obrzud, S. Lecomte, and T. Herr, Temporal solitons in microresonators driven by optical pulses, Nat. Photonics **11**, 600 (2017).

[15] Z. Kang, F. Li, J. Yuan, K. Nakkeeran, J. N. Kutz, Q. Wu, C. Yu, and P. K. A. Wai, Deterministic generation of single soliton Kerr frequency comb in microresonators by a single shot pulsed trigger, Opt. Express **26**, 18563 (2018).

[16] V. Brasch, E. Obrzud, S. Lecomte, and T. Herr, Nonlinear filtering of an optical pulse train using dissipative Kerr solitons, Optica **6**, 1386 (2019).

[17] J. K. Jang, M. Erkintalo, S. Coen, and S. G. Murdoch, Temporal tweezing of light through the trapping and manipulation of temporal cavity solitons, Nat. Commun. **6**, 7370 (2015).

[18] I. Hendry, W. Chen, Y. Wang, B. Garbin, J. Javaloyes, G.-L. Oppo, S. Coen, S. G. Murdoch, and M. Erkintalo, Spontaneous symmetry breaking and trapping of temporal Kerr cavity solitons by pulsed or amplitude-modulated driving fields, Phys. Rev. A **97**, 053834 (2018).

[19] N. Lilienfein, C. Hofer, M. Högner, T. Saule, M. Trubetskov, V. Pervak, E. Fill, C. Riek, A. Leitenstorfer, J. Limpert, F. Krausz,

and I. Pupeza, Temporal solitons in free-space femtosecond enhancement cavities, Nat. Photonics **13**, 214 (2019).

[20] M. Erkintalo, S. G. Murdoch, and S. Coen, Phase and intensity control of dissipative Kerr cavity solitons, J. R. Soc. N. Z. **52**, 149 (2022).

[21] A. Pikovsky, M. Rosenblum, and J. Kurths, *Synchronization: A Universal Concept in Nonlinear Sciences* (Cambridge University Press, Cambridge, 2001).

[22] Q.-F. Yang, X. Yi, K. Y. Yang, and K. Vahala, Counter-propagating solitons in microresonators, Nat. Photonics **11**, 560 (2017).

[23] C. Joshi, A. Klenner, Y. Okawachi, M. Yu, K. Luke, X. Ji, M. Lipson, and A. L. Gaeta, Counter-rotating cavity solitons in a silicon nitride microresonator, Opt. Lett. **43**, 547 (2018).

[24] J. K. Jang, A. Klenner, X. Ji, Y. Okawachi, M. Lipson, and A. L. Gaeta, Synchronization of coupled optical microresonators, Nat. Photonics **12**, 688 (2018).

[25] J. K. Jang, X. Ji, C. Joshi, Y. Okawachi, M. Lipson, and A. L. Gaeta, Observation of arnold tongues in coupled soliton Kerr frequency combs, Phys. Rev. Lett. **123**, 153901 (2019).

[26] I. Aranson, K. Gorshkov, A. Lomov, and M. Rabinovich, Stable particle-like solutions of multidimensional nonlinear fields, Physica D **43**, 435 (1990).

[27] W. J. Firth and A. J. Scroggie, Optical bullet holes: Robust controllable localized states of a nonlinear cavity, Phys. Rev. Lett. **76**, 1623 (1996).

[28] S. Longhi, Perturbation of parametrically excited solitary waves, Phys. Rev. E **55**, 1060 (1997).

[29] I. V. Biktasheva, Yu. E. Elkin, and V. N. Biktashev, Localized sensitivity of spiral waves in the complex Ginzburg-Landau equation, Phys. Rev. E **57**, 2656 (1998).

[30] M. Tlidi, A. Vladimirov, and P. Mandel, Interaction and stability of periodic and localized structures in optical bistable systems, IEEE J. Quantum Electron. **39**, 216 (2003).

[31] A. J. Scroggie, J. Jeffers, G. McCartney, and G.-L. Oppo, Reversible soliton motion, Phys. Rev. E **71**, 046602 (2005).

[32] J. P. Mizrahi, D. Zilberg, and O. Gat, Universal dynamics of spatiotemporal entrainment with phase symmetry, Phys. Rev. E **108**, 014120 (2023).

[33] I. V. Barashenkov and Yu. S. Smirnov, Existence and stability chart for the ac-driven, damped nonlinear Schrödinger solitons, Phys. Rev. E **54**, 5707 (1996).

[34] H. A. Haus and Y. Lai, Quantum theory of soliton squeezing: A linearized approach, J. Opt. Soc. Am. B **7**, 386 (1990).